Friction **11**(1): 48–63 (2023)
https://doi.org/10.1007/s40544-021-0571-8
ISSN 2223-7690
CN 10-1237/TH
RESEARCH ARTICLE

Study on the mechanism of rapid formation of ultra-thick tribofilm by CeO_2 nano additive and ZDDP

Xue LEI, Yujuan ZHANG*, Shengmao ZHANG*, Guangbin YANG, Chunli ZHANG, Pingyu ZHANG

National & Local Joint Engineering Research Center for Applied Technology of Hybrid Nanomaterials, Henan University, Kaifeng 475004, China

Received: 24 August 2021 / Revised: 19 October 2021 / Accepted: 11 November 2021

Abstract: CeO_2 nanoparticles are potential anti-wear additives because of their outstanding anti-wear and load-bearing capacity. However, the shear-sintering tribo-film formation mechanism of oxide nanoparticles limits the tribo-film formation rate and thickness greatly. In this study, by compounding with zinc dioctyl dithiophosphate (ZDDP), ultra-fine CeO_2 nanoparticles modified with oleylamine (OM) can quickly form 2 μm ultra-thick tribo-film, which is 10–15 times thicker than that of ZDDP and CeO_2, respectively. The ultra-thick tribo-film presents a nanocomposite structure with amorphous phosphate as binder and nano-CeO_2 as filling phase, which leads to the highest loading capacity of composite additives. The results of adsorption experiments tested by dissipative quartz crystal microbalance (QCM-D) showed that the P_B value of additive has nothing to do with its equilibrium adsorption mass, but is directly proportional to its adsorption rate in 10 s. The compound additive of CeO_2 and ZDDP presented the co-deposition mode of ZDDP monolayer rigid adsorption and CeO_2 viscoelastic adsorption on the metal surface, which showed the highest adsorption rate in 10 s. It is found that the tribo-film must have high film forming rate and wear resistance at the same time in order to achieve super thickness. Cerium phosphate was formed from ZDDP and CeO_2 through tribochemistry reaction, which promotes the formation of an ultra-thick tribo-film with nanocomposite structure, which not only maintains the low friction characteristics of CeO_2, but also realizes high P_B and high load-carrying capacity.

Keywords: CeO_2 nanoadditives; adsorption; nanocomposite ultra-thick tribofilm; zinc dioctyl dithiophosphate (ZDDP)

1 Introduction

As lubricating additives of lubricating oil, nanoparticles have shown super extreme pressure [1, 2], self-repairing [3], outfield responsiveness [4, 5], and many other excellent performances. The excellent performance of nano-additives is based on the tribo-film with high performance formed under the mechanochemical action of sliding interface. However, for nanoparticle additives, both the shear-sintering tribo-film formation mechanism of metal [6] and oxide nanoparticles [7] and the graphitization tribo-film formation mechanism of carbon nanoparticles (graphene, carbon quantum dots, and fullerene) [8–10] often lead to long induced growth period and low film formation rate. Even if the tribo-film with high bearing capacity and good wear resistance is eventually formed, it has already caused damage to the mechanical surface during the induction period of the formation of the tribo-film. Therefore, the promising lubricating additives should not only be able to form the tribo-film with high strength and low shear, but also have high film-forming rate. The results of our previous study show that oleylamine (OM) modified CeO_2 nanoparticles (with an average particle size of 4.5 nm) showed outstanding anti-wear and load-bearing capacity at the concentration

* Corresponding authors: Yujuan ZHANG, E-mail: cnzhangyujuan@henu.edu.cn; Shengmao ZHANG, E-mail: zsm@vip.henu.edu.cn

of 0.2%, but the P_B value is far lower than zinc dioctyl dithiophosphate (ZDDP), which is widely used as an anti-wear additive [11].

The maximum non-seizure load P_B (measured at 1,770 rpm, 25 °C, and 10 s, according to the ASTM D2783-98) is an important index to evaluate the extreme pressure performance of additives, which evaluates whether additives can form a protective tribo-film on the friction surface within 10 s, that is, whether the additive can form anti-wear tribo-film under the shear induction of less than 300 times. It is reported that the crystal phase tribo-film formed by oxide nanoparticles as the anti-wear additive of PAO6 oil under the shear induction of AFM tip has much higher hardness and elastic modulus than that of ZDDP, but 3,000 times of shear induction are required to start nucleation and growth，the thickness of tribo-film finally stablilized at 60 nm [7]. ZDDP is the most widely used anti-wear additive, and tribo-film with amorphous polyphosphate can be formed under the action of stress-assisted and thermally activated chemical reactions [12]. Although ZDDP can rapidly form anti-wear tribo-film within hundreds of shear, and has a high P_B value, the load-carrying capacity of amorphous polyphosphate structure tribo-film formed by ZDDP is much lower than that of the sintered crystalline phase tribo-film formed by oxide nano additives. Therefore, the final thickness of the tribo-film is stable at 40 nm [13]. It can be seen that high load-carrying capacity or tribo-film formation rate alone can't form ultra-thick tribo-film, and cannot achieve rapid and long-term protection of friction surface.

Although the idea of combining the advantages of small molecule additives and nano additives is attractive, the related research results are complex and diverse. On the one hand, small molecule additives can participate in the friction reaction of nano additives and produce beneficial effects. For example, ZDDP can participate in the tribochemistry reaction of Cu nanoparticles [14] and WS_2 nanoparticles [15] through the sulfur released by the tribochemistry reaction, which can inhibit the oxidation of nanoparticles. On the other hand, the researchers found that the effective adsorption of additives on the surface of the friction pair is the premise of producing efficient lubrication performance through quartz crystal microbalance (QCM) adsorption experiment [4, 5]. However, the strong competitive adsorption of small molecule additives and nano additives will hinder the effective adsorption of nano additives on the friction surface and make them unable to play a role [16]. Therefore, how to combine the excellent friction reducing, anti-wear, and bearing capacity of CeO_2 with the advantages of rapid tribo-film-forming of ZDDP to optimize the microstructure of ZDDP and CeO_2 tribo-film, and finally protect the friction surface quickly and effectively for a long time is an urgent subject to be studied.

In this study, the effects of CeO_2 nanoparticles and ZDDP as composite additives on the friction reduction, anti-wear, extreme pressure resistance, and load-bearing capacity of lubricating oil PAO6 were studied. The adsorption behavior of the two on the metal surface was studied by dissipative quartz crystal microbalance (QCM-D), and the effects of adsorption rate and equilibrium adsorption mass on P_B value, wear resistance, and loading capacity were also studied. The composition and microstructure of tribo-film were analyzed by focused ion beam (FIB), energy-dispersive X-ray spectroscopy (EDS), and X-ray photoelectron spectroscopy (XPS). The mechanism of the synergistic effect of the two on the film forming rate and tribological properties of tribo-film was studied.

2 Experimental

2.1 Materials

The CeO_2 nanoparticles used in this study were synthesized according to the steps reported in Ref. [17]. Since the modifier used is oleylamine (OM), it is hereinafter referred to as OM modified-CeO_2 nanoparticles. The size distribution diagram of these nanoparticles shows that the average particle size of CeO_2 nanoparticles is in the range of 4–6 nm (see Fig. S1 in the Electronic Supplementary Material (ESM)). The base oil used in this paper is poly-alpha olefin (PAO6), which was provided by Shandong Qingdao Lubricating Materials Co., Ltd., and the relevant parameters are shown in Table S1 in the ESM. Petroleum ether (analytical pure) were purchased from Tianjin Fuyu Fine Chemical Co., Ltd. The ZDDP

used was provided by Jinzhou Kangtai Lubricant Additive Co., Ltd. (Liaoning, China). All the chemicals used were not further purified, and the test water was distilled water.

2.2 Dispersion performance of OM-modified CeO_2 nanoparticles in PAO6 and preparation of lubricants

The oil samples of 0.2 wt% was prepared by adding OM-modified CeO_2 nanoparticles into PAO6. After ultrasonic dispersion for 10 min, the oil sample was shaken evenly. After standing for 12 hours, the stability of CeO_2 nanoparticles in PAO6 was tested by stability analyzer (LUM Lumisizer 651) at 4,000 rpm for 3,000 s. The dispersion stability of CeO_2 nanoparticles in PAO6 is good, and the specific results are shown in Fig. S2 in the ESM.

The samples were uniformly dispersed after ultrasonic treatment for 10 min. The specific concentration of CeO_2 nanoparticles and ZDDP (zinc dioctyl dithiophosphate, T203, Jinzhou Kangtai Lubricating Oil Additive Co., Ltd.) is shown in Table 1. Among them, the additive concentration of CeO_2 nanoparticles is the best concentration obtained through tribology tests (Fig. S3 in the ESM), and the additive concentration of ZDDP is the middle value of the optimal additive range recommended by the manufacturer.

2.3 Tribology tests

A four-ball friction tribometer (Xiamen Tianji Automation Co., Ltd.) was used to test the tribological properties and the P_B of the additive mixed with PAO6. GCr15 steel balls (Shanghai Steel Ball Co., Ltd., China) with an elastic modulus of 208 GPa and a Poisson's ratio of 0.30 were used as the friction pair. The friction and wear tests were as follows: 1,200 rpm, load 392 N, 75 °C, 60 min. Each test was repeated three times. The specific process refers to four ball test standard ASTM D2266-01. The P_B was tested at 1,770 rpm, 25 °C, and 10 s according to the GB/T 12583-98 (refer to ASTM D2783-98). Each test was repeated three times. After the test, the wear spot diameter (WSD) of three lower balls was measured with the optical microscope (accuracy ± 0.01 mm). The coefficient of friction (COF) was based on the computer output of the testing machine.

Table 1 Abbreviated form and the corresponding added concentration of the prepared nano-lubricant/adsorption test sample.

Abbreviated form	ZDDP (wt%)	OM-modified CeO_2 (wt%)
PAO6/dodecane+CeO_2	—	0.2
PAO6/dodecane+ZDDP	1.75	—
PAO6/dodecane+ZDDP+CeO_2	1.75	0.2

Load-bearing capacity of lubricant was performed on a UMT-5 tribometer (UMT-TriboLab, Bruker, USA) using a ball-on-flat reciprocating sliding configuration. The upper specimen was GCr15 steel ball with a diameter of 12.7 mm, the lower specimen is made of GCr15 stainless steel with the specification of 40 mm × 30 mm × 5 mm. A continuous loading mode was used from 100 to 1,800 N at the speed of 50 N every 3 min, before continuous loading, it was set to run in for 10 minutes at 100 N. Each test was repeated three times.

2.4 Surface characterization of wear scar

A scanning electron microscope (SEM, Carl Zeiss) equipped with energy dispersive spectrometer (EDS) accessories was performed to analyze the morphology of worn surfaces and the distribution of tribo-film elements. The three-dimensional (3D) morphology of the worn surface was obtained by contour GT-I white-light interfering profilometer (Bruker, Germany). A focused ion beam (FIB) system was used to extract the cross-section of the tribo-film in the middle part of the wear scar of the steel ball. In order to ensure the integrity of the surface structure of the wear mark, a layer of Pt protective layer was sprayed on the surface of the wear spot before using the FIB system. The structure and chemical composition of the tribo-film were studied by transmission electron microscopy (TEM, JEM-2100, Japan) and energy dispersive X-ray spectroscopy (EDS). In order to further determine the element composition and chemical state of the tribo-film on the worn surface, X-ray photoelectron spectroscopy (XPS, PHI-5702, American Electronic Physics Corporation) test was carried out on the worn surface.

2.5 Adsorption behavior test

QCM-D is a kind of sensor based on the piezoelectric

effect of crystal, which can not only detect the change of vibration frequency (Δf) of wafer caused by additive adsorption, but also give the change of dissipation factor (ΔD) of adsorption film. The adsorption behaviors of additive on the wafer can be obtained by analyzing Δf of wafer and ΔD of the additive adsorption layer [18, 19]. Due to the high viscosity of PAO6, it is impossible to pass QCM-D flow pool. Dodecane, which has the same saturated alkyl chain as the PAO6 molecular structure but lower viscosity, was selected as the base oil for the adsorption experiment. The concentration of CeO_2 nanoparticles and ZDDP was the same as that of tribological test, refer to Table 1 for details. The experimental process was as follows: before the experiment, the sample tank and pipeline were cleaned with washing solution, and nitrogen was used for purging and drying. Firstly, a clean gold-plated wafer was installed in the QCM-D device (QSense Explorer Extreme Temperatures, Biolin, Finland), after the instrument was connected, dodecane was introduced as the baseline and stabilized for 10–15 minutes until the fluctuation of Δf value did not exceed 2 Hz, subsequently, the prepared sample solution was introduced, and keep the adsorption for about 3 hours. All the measurements were conducted at 25 °C and a flow rate of 80 μl/min.

3 Results

3.1 Tribological properties of CeO_2 nanoparticles and ZDDP in PAO6

The evolution of friction coefficients (COF) as a function of time for PAO6, PAO6+CeO_2, PAO6+ZDDP, and PAO6+ZDDP+CeO_2 is shown in Fig. 1(a). The COF of PAO6 fluctuated greatly within 1 h, gradually increasing from 0.061 to 0.081, which indicates that PAO6 cannot form a sufficient protective layer on the friction surface without additives, and the increasing wear surface (see Fig. 1(b)) will continue to increase the COF due to the adhesion and debris. The COF of ZDDP was 31.5% higher than that of pure PAO6. This result is similar to that reported by the Spikes research group [20, 21], and the tribo-film formed by ZDDP usually exhibits a higher COF. The COF of PAO6+ZDDP+CeO_2 decreased to the same level as PAO6+CeO_2, while the friction curve was more stable than that of PAO6+CeO_2. It indicates that the tribo-film formed by the combination of CeO_2 nanoparticles and ZDDP has higher structural stability. As shown in Fig. 1(b), ZDDP has a certain anti-wear performance, which is similar to the results reported previously [22], but the WSD of CeO_2 nanoparticles was significantly lower than that of ZDDP, while WSD of PAO6+ZDDP+CeO_2 exhibited the best anti-wear performance, which showed 56.8% reduction in WSD compared to pure PAO6. The results show that ZDDP and CeO_2 nanoparticles have favorable synergistic effect on improving the friction reducing and anti-wear properties of PAO6 base oil.

P_B value is an important index to evaluate the extreme pressure performance of additives, which evaluates whether the additive can form a protective tribo-film on the friction surface within 10 s. As shown in Fig. 2, the P_B value of PAO6+CeO_2 is not ideal, CeO_2 nanoparticles failed to form an effective anti-wear tribo-film within 10 s, and the extreme pressure performance was the same as that of PAO6.

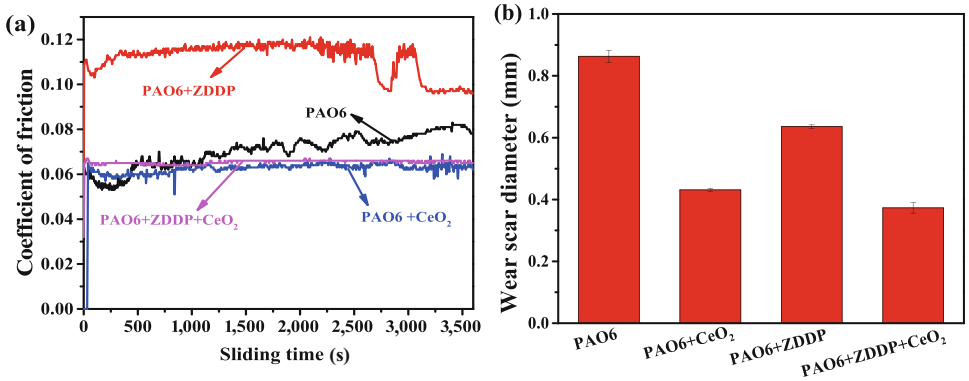

Fig. 1 Tribological properties of CeO_2 nanoparticles and ZDDP in PAO6: (a) coefficient of friction–time curve, (b) average wear scar diameter (four-ball tribometer: 1,200 rpm, 392 N, 75 °C, 60 min).

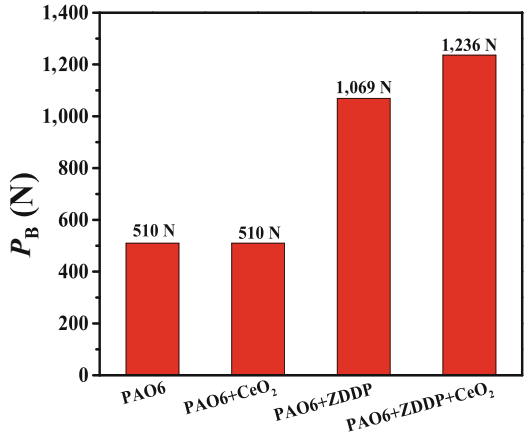

Fig. 2 P_B values of various lubricants (four-ball friction and wear tester, 1,750 rpm, 10 s).

The P_B value of PAO6+ZDDP reached 1,098 N, which was 15 levels higher than that of PAO6. It shows that ZDDP can form an effective anti-wear tribo-film within 10 s, that is, less than 281 shear induction, and its tribo-film forming rate is much higher than that of CeO_2 nanoparticles. The results are consistent with those reported in Refs. [7, 13, 20]. ZDDP can form tribo-film under hundreds of shear induction, while oxides can form tribo-film only after 3,000 shear induction. It can be seen that the higher the film forming rate is, the greater the P_B value is. The P_B value of PAO6+ZDDP+CeO_2 was further increased by 2 levels compared with that of PAO6+ZDDP, which indicates that, under the tribochemistry induction of ZDDP, CeO_2 nanoparticles not only participated in the formation of tribo-film, but also improved the load-bearing capacity and anti-wear performance of tribo-film. The increase of P_B value of compound additive of ZDDP+CeO_2 is not only related to the tribo-film forming rate of additives, but also to the bearing capacity of tribo-film. Therefore, to determine the contribution of CeO_2 nanoparticles to P_B value, it is necessary to further study the bearing capacity and formation rate of the tribo-film.

In order to verify the load-bearing capacity of ZDDP, CeO_2, and ZDDP+CeO_2, a continuous loading experiment under reciprocating mode was carried out on UMT-5 friction testing machine. After pre-grinding for 10 minutes, a stable tribo-film was formed, and the load-bearing capacity of PAO6, PAO6+CeO_2, PAO6+ZDDP, and PAO6+CeO_2+ZDDP was compared by continuous loading experiments. As shown in Fig. 3, the load-bearing capacity of PAO6 was relatively poor, and the COF increased gradually with the increase of load. When the load reached 600 N, the COF suddenly increased and reached the load-bearing limit. The COF of PAO6+ZDDP had a tendency to increase in the early stage, and gradually stabilized after 1,500 s, but the COF was higher overall, and the maximum load did not exceed 900 N, indicating that the load-bearing capacity of ZDDP is not prominent. During the whole process of pre-grinding and loading, the COF of PAO6+CeO_2 is stable and lower than that of ZDDP by 25%, and the maximum load is 1,650 N. It can be seen that, although the formation rate of CeO_2 tribo-film is slow, once formed, the load-carrying capacity of the shear sintered crystalline oxide tribo-film is much higher than that of the amorphous polyphosphate tribo-film formed by ZDDP [20, 23]. Interestingly, the COF of PAO6+ZDDP+CeO_2 was relatively large in the early stage, which was equivalent to PAO6+ZDDP. With the steady increase of load, COF gradually decreases and remains stable. The stable COF is almost the same as that of PAO6+CeO_2. The tribological behaviors of CeO_2 and ZDDP composite additives are different from that of ZDDP and CeO_2 alone, but a combination of them. The load-carrying capacity of the tribo-film of the composite additive is 1,700 N, which is more than that of the two single additives. Therefore, the tribo-film microstructure of the composite additive should be neither amorphous polyphosphate nor crystalline oxide. The tribo-film formed by CeO_2 and ZDDP composite additive has high P_B value and high load-carrying capacity at the

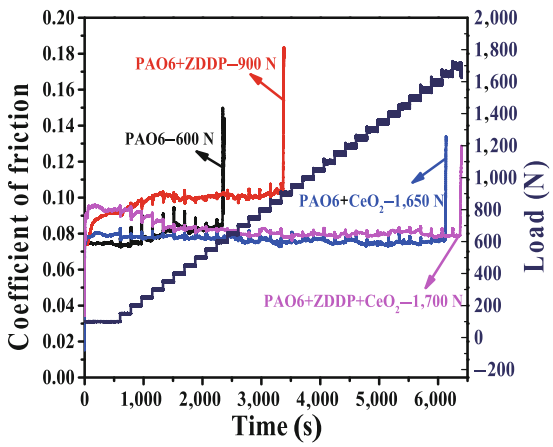

Fig. 3 Time-dependent coefficient of friction of different lubricants under continuous loading (UMT-5).

same time, which proves that its tribo-film-forming rate and mechanical properties are better than that of any single additive. Further analysis of the tribo-film is needed to reveal the synergistic effect between ZDDP and CeO_2.

3.2 Analysis of wear surface

The SEM micrographs and 3D profiles of the wear scar lubricated with pure PAO6, PAO6+CeO_2, PAO6+ZDDP, PAO6+ZDDP+CeO_2 are shown in Fig. 4. As shown in Fig. 4(a), the wear scar lubricated with pure PAO6 was the largest. It is obvious from the 3D profiles that the furrows on the worn surface were wide and deep. Compared with Fig. 4(b), the WSD of PAO6+CeO_2 was much smaller, and the furrows on the worn surface are shallower, and more furrows may be caused by abrasive wear. The worn surface of PAO6+ZDDP was reduced to a certain extent compared with PAO6, but the deeper furrows could be observed from the SEM and 3D profiles of Fig. 4(c), the WSD of PAO6+ZDDP+CeO_2 was the smallest and smoothest, more prominent is the formation of a complete round pad like tribo-film (Fig. 4(d)).

Figure 5 shows 2D images of the worn surface of PAO6, PAO6+CeO_2, PAO6+ZDDP, and PAO6+ZDDP+CeO_2. The wear of PAO6 and PAO6+ZDDP is large, which leads to the wear spot depression. Once CeO_2 nanoparticles form a tribo-film, it will show outstanding anti-wear ability, so the wear scar is flat. For the composite additives, the wear scar not only does not sink, but also is 2.01 μm higher than the wear scar surface. The thickness of the tribo-film is much higher than the typical thickness of ZDDP tribo-film reported in Ref. [24]. It has been found that the growth and wear of the tribo-film occur simultaneously. In the AFM *in-situ* growth experiment, the tribo-film thickness formed by ZDDP based on the stress and thermal activation mechanism was finally stabilized at 40 nm [7]. Similarly, the thickness of the tribo-film formed by ZrO_2 nanoparticles based on the shear sintering mechanism was finally stabilized at 60 nm in the AFM *in-situ* growth experiment [13]. The final thickness

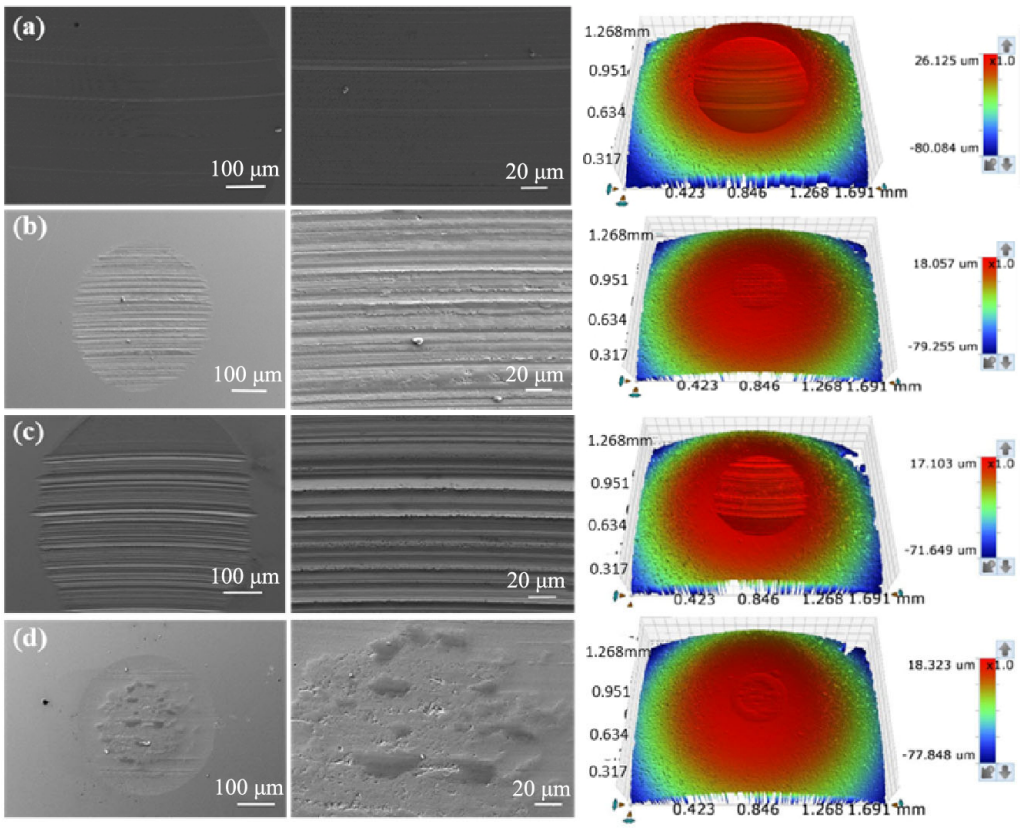

Fig. 4 SEM micrographs and 3D profiles of worn steel surfaces lubricated by (a) PAO6, (b) PAO6+CeO_2, (c) PAO6+ZDDP, (d) PAO6+ZDDP+CeO_2 (four-ball tribometer: 1,200 rpm, 392 N, 75 °C, 60 min).

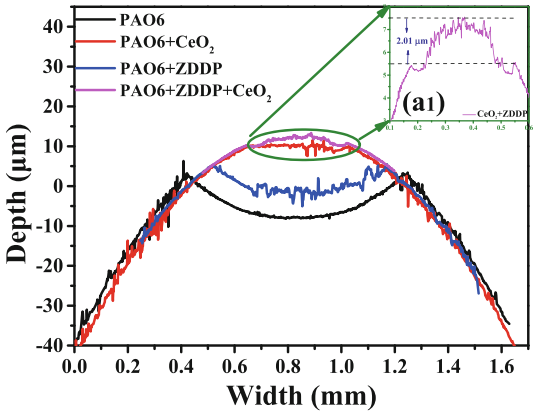

Fig. 5 2D image of the worn steel surfaces lubricated by PAO6+ZDDP+CeO_2.

of the tribo-film depends on the formation rate and anti-wear ability of tribo-film. According to the previous experimental results in this paper, although ZDDP has high film-forming rate, which leads to high P_B value, its anti-wear ability is poor, so the wear scar is large and obviously concave, and no obvious tribo-film is observed in Fig. 5. For composite additive, it has both high film formation rate and wear resistance, that is, in the growth stage of tribo-film, the growth rate of the tribo-film is far greater than its wear rate, resulting in the rapid formation of ultra-thick tribo-film, and finally the tribo-film is stable at 2 μm.

In order to detect the composition of the tribo-film, the surface distribution of typical elements was studied. As shown in Fig. 6(a), the PAO6 lubricated worn surface is only enriched in O elements, which corresponds to the oxidation caused by friction heat. Without the participation of additives, the intense friction caused by direct adhesion between steel balls leads to a large amount of friction heat, which leads to oxidation of surface, the formation of oxide film greatly reduces the surface energy of friction surface, and reduces the COF to a certain extent. However, the low load-carrying capacity of the amorphous oxide leads to the maximum WSD. The distribution of Zn and P is the most significant on the wear surface of PAO6+ZDDP, while the distribution of S element is less on the wear surface (Fig. 6(c)). According to Refs. [7, 11, 25], the ZDDP tribo-film is mainly composed of zinc phosphate, iron phosphate, and iron oxide, and only contains a small amount of sulfide at the interface. In the tribochemical reaction, a large amount of sulfur in ZDDP is decomposed and released in the form of alkyl mercaptan, and rarely remains in the tribo-film, which is consistent with the composition of ZDDP tribo-film in this study. Obvious enrichment of O and Ce elements is found on the worn surface of PAO6+CeO_2 (Fig. 6(b)), which is shear sintered tribo-film on the worn surface [17, 23]. However, in the worn surface of PAO6+CeO_2+ZDDP, as shown in

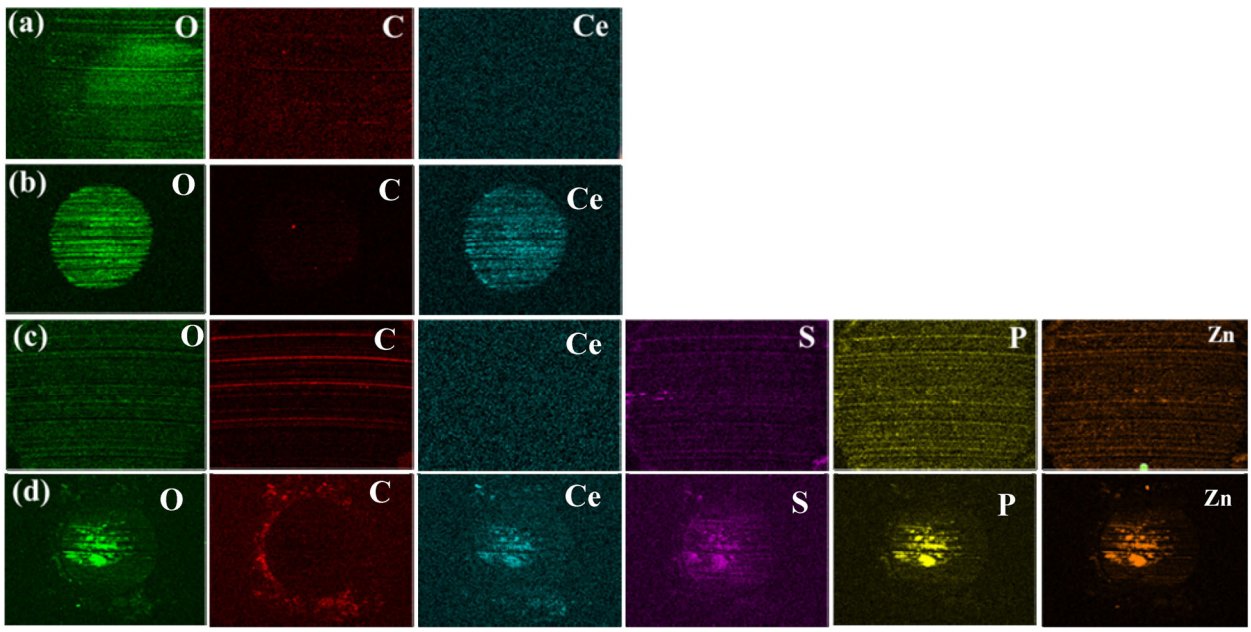

Fig. 6 EDS maps of the worn steel surfaces lubricated by (a) PAO6, (b) PAO6+CeO_2, (c) PAO6+ZDDP, (d) PAO6+ZDDP+CeO_2 (four-ball tribometer: 1,200 rpm, 392 N, 75 °C, 60 min).

Fig. 6(d), it contains not only the typical elements of CeO_2, but also the typical elements of ZDDP, and the distribution position overlaps completely. At the same time, it is found that the enrichment of S in the tribo-film is far more obvious than that of ZDDP tribo-film. Therefore, CeO_2 and ZDDP contribute to the formation of tribo-film at the same time, the participation of CeO_2 nano additives changed the tribochemistry reaction of ZDDP, which resulted in a new film forming mechanism and structure instead of simply superposition of CeO_2 tribo-film and ZDDP tribo-film.

3.3 Compatibility mechanism

3.3.1 Study on adsorption behavior

In order to analyze the relationship between the adsorption behavior of additives and their tribological properties, the adsorption behavior of CeO_2, ZDDP, and CeO_2+ZDDP in dodecane was tested by QCM-D. Figure 7 shows the curves of Δf and ΔD of the three kinds of additives. First, the adsorption capacity of ZDDP is very weak, its Δf of equilibrium adsorption is less than 12 Hz, corresponding to its lower equilibrium adsorption mass (Fig. 8(b)). However, the adsorption equilibrium of ZDDP was reached quickly within 20 s. For CeO_2 nanoparticles, the Δf of equilibrium adsorption is as high as 300 Hz, corresponding to its higher equilibrium adsorption mass (Fig. 8(b)). Because the particle size of CeO_2 nanoparticles is much larger than that of ZDDP, the diffusion ability of CeO_2 nanoparticles in base oil is greatly reduced, and the adsorption equilibrium is reached in nearly 10,000 s (Fig. 7(a)). The Δf of ZDDP+CeO_2 is almost the same as that of CeO_2, but it took only 2,000 s for ZDDP+CeO_2 to reach the adsorption equilibrium, which is one fifth of that of CeO_2. This means that ZDDP promotes the adsorption rate of CeO_2. It should be noted that, as shown in Fig. 7(b), ZDDP is a dense rigid adsorption layer. The

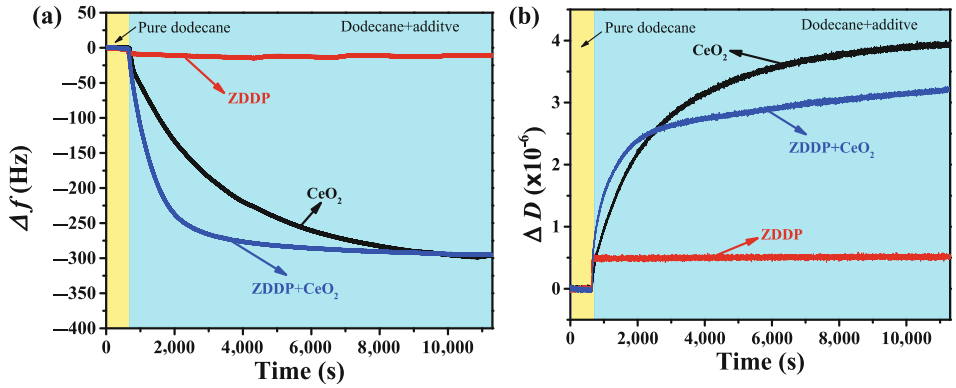

Fig. 7 Changes in the adsorption behavior of CeO_2, ZDDP, ZDDP+CeO_2 (dodecane solution) on metal surfaces: (a) frequency change (Δf) curve, (b) energy dissipation factor change (ΔD) curve.

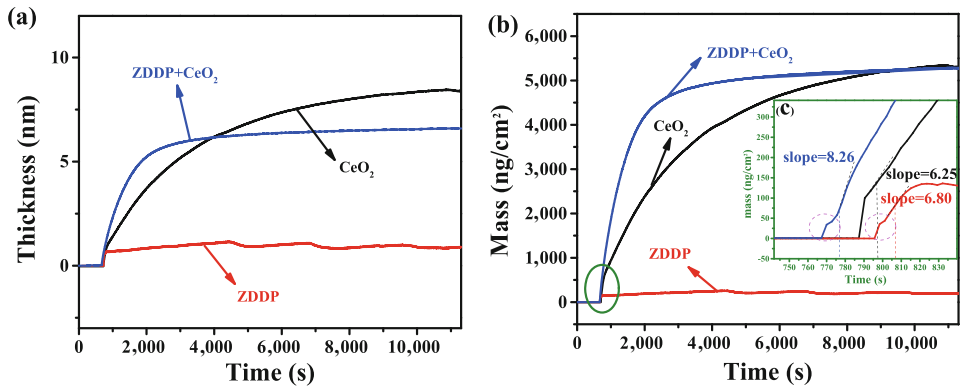

Fig. 8 Change curve of adsorption behavior of CeO_2, ZDDP, and CeO_2+ZDDP on gold-plated wafers: (a) adsorption film thickness and (b) deposition quality/cm^2; (c) is partial enlarged views of (b).

hydrophobic association between the straight chain alkanes in ZDDP molecules makes it form a dense monolayer adsorption with regular structure [26], so its ΔD is lower than 1×10^{-6}. The ΔD of CeO_2 is higher than 1×10^{-6}, which is typical viscoelastic adsorption. Although CeO_2 surface modifier is a straight-chain alkylamines, because it is connected with CeO_2, it not only limits the rotation and arrangement of its molecular chains, but also causes steric hindrance to the arrangement of inorganic nuclei, as a result, the density of the adsorption layer decreases and a viscoelastic adsorption layer is formed. The ΔD of ZDDP+CeO_2 is between that of ZDDP and CeO_2, because of the existence of ZDDP, the adsorption film structure of ZDDP+CeO_2 is more compact than that of single CeO_2, and presented a composite structure of ZDDP single rigid adsorption layer and CeO_2 viscoelastic adsorption layer.

For further analyzing the relationship between the adsorption behavior and the tribological properties, the Q-Sense Dfind software was used to fit the data in Fig. 7 to obtain the adsorption layer thickness and the deposition mass per cm^2, as shown in Figs. 8(a) and 8(b). Among them, rigid adsorption layer and viscoelastic adsorption layer should be calculated by different formulas. The ΔD of ZDDP adsorption layer is less than 1×10^{-6}, which belongs to rigid adsorption. Its adsorption layer thickness and adsorption mass per unit area are calculated by Sauerbrey model. The ΔD of CeO_2 and ZDDP+CeO_2 adsorption layers is greater than 1×10^{-6}, which belong to typical viscoelastic adsorption. Their adsorption layer thickness and adsorption mass per unit area are calculated by Dfind Smartfit model [27, 28]. Figure 8(a) shows that the adsorption film of ZDDP is relatively thin, with an average of about 1.5 nm, which is consistent with the molecular size of ZDDP calculated by Materials Studio software, so the ZDDP adsorption layer belongs to single molecular layer adsorption. At the same time, ZDDP shows the lowest equilibrium adsorption mass (ng/cm^2) in Fig. 8(b). The adsorption layer thickness of CeO_2 nanoparticle is 8.3 nm, according to the particle size distribution of CeO_2 nanoparticles (Fig. S1(e) in the ESM), it can be inferred that CeO_2 nanoparticles adsorbed about 2 layers on the wafer. However, when CeO_2 and ZDDP coexist, the equilibrium adsorption mass is similar to that of CeO_2, but the thickness of the adsorption layer is only 6.5 nm. Therefore, compared with CeO_2 adsorption layer, the composite additive adsorption layer is more compact, corresponding to its lower ΔD. When exploring the relationship between equilibrium adsorption mass and P_B value of three additives, it was found that P_B value of ZDDP with the lowest equilibrium adsorption mass was much higher than that of CeO_2, whose equilibrium adsorption mass was 26 times that of ZDDP. However, the P_B values of CeO_2 and CeO_2+ ZDDP with almost the same equilibrium adsorption mass differ by 18 levels, which shows that there is no direct relationship between P_B value and equilibrium adsorption mass.

Since the P_B value is the protection ability of additives in 10 s, the adsorption rates of CeO_2, ZDDP, and ZDDP+CeO_2 in 10 s were compared. A piece of data (one part of the curve was marked with circle) at the beginning of the adsorption curves in Fig. 8(b) was intercepted to obtain Fig. 8(c). In order to obtain the adsorption rates of CeO_2, ZDDP, and ZDDP+CeO_2 more intuitively, tangent lines were made at the 10th second of the beginning of adsorption behavior for different additives in Fig. 8(c). At this time, the slope of CeO_2+ZDDP is the largest, followed by ZDDP, and CeO_2 is the smallest. Therefore, at the 10th second, the adsorption rate of CeO_2+ZDDP is the highest, followed by ZDDP, and CeO_2 is the lowest, and the adsorption rate of CeO_2+ZDDP in the 10th second is 32.16% higher than that of CeO_2 alone. It can be found that the adsorption rate of the three additives in the 10th second is directly proportional to their P_B value in Fig. 2. This shows that the adsorption rate of additives is positively related to the formation rate of tribo-film on the worn surface, and the formation rate of tribo-film is directly proportional to the P_B value.

On the other hand, the sensitivity of QCM-D is extremely high. The trend of the two parts of the curve circled by the dotted line in Fig. 8(c) is quite consistent, this means that the adsorption behavior of CeO_2+ZDDP and ZDDP is consistent in the initial stage of adsorption behavior. In other words, when CeO_2 nanoparticles and ZDDP coexist, the ZDDP molecules preferentially adsorb a layer on the metal surface. Subsequently, the polar ends of the remaining ZDDP molecules will adsorb on the surface of the CeO_2 nanoparticles, which promotes the CeO_2 nanoparticles

to adsorb faster, forming a denser adsorption film. This result is consistent with the conclusion drawn in Fig. 3.

3.3.2 *Composition analysis of tribo-film*

EDS results showed that CeO_2 participated in the tribochemistry reaction of ZDDP. In order to further explore the composition of the tribo-film formed by the composite additives, XPS analyses were performed on the wear scars for PAO6+CeO_2, PAO6+ZDDP, PAO6+ZDDP+CeO_2. The element percentage content of the characteristic elements on the surface of the wear scar is shown in Table 2. It is worth noting that the content of Ce, Zn, S, and P in the worn surface of PAO6+CeO_2+ZDDP steel balls is much higher than PAO6+CeO_2 and PAO6+ZDDP. This means that after the combination of CeO_2 nanoparticles and ZDDP, the amount of the two involved in the tribochemistry reaction increases, which is also the reason for the formation of a thicker tribo-film.

Figure 9 shows the XPS spectra of the characteristic elements after etching on the worn surface of the steel ball of PAO6+CeO_2, PAO6+ZDDP, and PAO6+CeO_2+ZDDP. As shown in Fig. 9(a), the peak of C 1s at 284.8 eV corresponds to the C–C bond [21]. The N 1s signal at 399.9 eV in Fig. 9(b) is mainly due to the adsorption of OM on the surface of CeO_2 nanoparticles to the worn surface. As shown in Fig. 9(c), the O 1s signal detected on the worn surface of PAO6+CeO_2+ZDDP has peaks at 529.6 eV, 530.2 eV, and 532.8 eV, corresponding to CeO_2, iron oxides, and metal phosphates [29]. The strength and proportion of phosphate in PAO6+CeO_2+ZDDP are much larger than those in PAO6+ZDDP, so it can be inferred that the participation of CeO_2 makes the tribochemistry reaction produce more phosphate. It can be seen from Fig. 9(d) that due to the high temperature and high pressure in the contact region, the Fe in the friction pairs is oxidized to form Fe_2O_3 and Fe_3O_4. At the same time, the signals of FeS (713.6 eV) were detected on the worn surfaces of PAO6+ZDDP and PAO6+CeO_2+ZDDP. In Fig. 9(f), the signal of metal sulfide on the worn surface of the PAO6+ZDDP is weak, and the peak of metal sulfate is relatively strong. However, the peak of metal sulfate on the worn surface of PAO6+CeO_2+ZDDP disappears, and the signal peak of metal sulfide is quite obvious [14]. This shows that the content of metal sulfide in the tribo-film is increased when CeO_2 nanoparticles are involved. The sulfate in the tribo-film is the product of sulfide after more intense shear oxidation. Metal sulfide is the main chemical state of sulfur in the tribo-film of PAO6+CeO_2+ZDDP, while metal sulfate is the main chemical state of sulfur in the ZDDP, which should be attributed to the high growth rate of the tribo-film of the PAO6+CeO_2+ZDDP to avoid the excessive shear oxidation of sulfide and the formation of sulfate. At the same time, metal sulfide has important role for protecting the steel surface from initial wear [30, 31]. The tribo-film formed by PAO6+ZDDP and PAO6+CeO_2+ZDDP contains a large amount of metal phosphates, as shown in Figs. 9(e) and 9(g), but the phosphate strength of PAO6+CeO_2+ZDDP tribo-film is obviously higher than that of PAO6+ZDDP tribo-film. The information from Ce 3d spectra shows that the signal peak of Ce 3d in the tribo-film of PAO6+CeO_2 is very weak, which is consistent with the results of previous study [17]. For this reason, the Ce 3d spectra of CeO_2 were inserted into Fig. 9(h) for comparison. It was found that the biggest difference of Ce 3d spectra in CeO_2 and tribo-film PAO+CeO_2+ZDDP was that obvious $CePO_4$ peak

Table 2 Percentage content of characteristic elements on steel ball wear spot.

Sample name		Element percentage content (%)							
		C 1s	N 1s	O 1s	Fe 2p	Zn 2p	S 2p	P 2p	Ce 3d
PAO6+CeO_2	Not etched	69.45	4.79	22.88	2.20	—	—	—	0.68
	Etched	67.64	3.91	24.67	2.68	—	—	—	1.10
PAO6+ZDDP	Not etched	75.07	—	20.18	1.68	0.71	1.02	1.34	—
	Etched	64.47	—	28.86	2.86	0.73	0.94	2.15	—
PAO6+CeO_2+ZDDP	Not Etched	38.53	3.65	34,63	1.63	5.85	2.97	11.40	3.66
	Etched	29.09	1.18	41.67	2.66	6.37	2.56	12.29	4.17

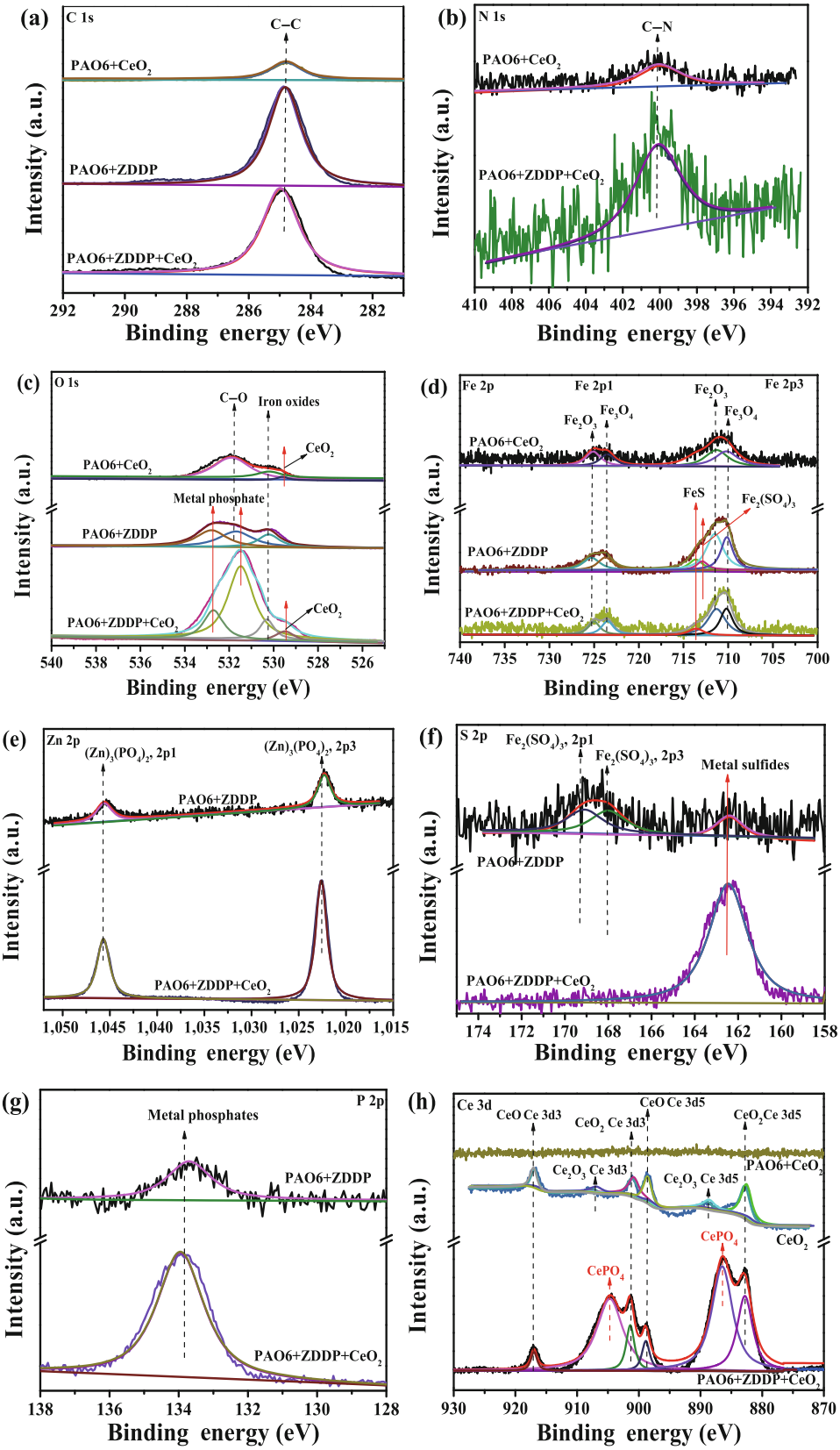

Fig. 9 XPS spectra of surface characteristic elements of wear scar surface of steel ball under lubrication of PAO6, PAO6+CeO_2, PAO6+ZDDP, and PAO6+CeO_2+ZDDP (four-ball tribometer: 1,200 rpm, 392 N, 75 °C, 60 min).

appeared in the PAO6+CeO_2+ZDDP tribo-film [32]. XPS analysis showed that a large amount of $CePO_4$ is formed by tribochemistry reaction between CeO_2 nanoparticles and ZDDP due to the high growth rate of the tribo-film, the sulfide in tribo-film is not transformed into sulfate by severe friction oxidation.

3.3.3 *Microstructure analysis*

In order to analyze the microstructure of the tribo-film, the cross-section sample of the tribo-film was extracted from the worn surface of steel ball lubricated with PAO6+CeO_2+ZDDP by using the FIB system. Figure 10(a) shows a cross-sectional TEM image of PAO6+ZDDP+CeO_2 tribo-film on the worn surface of steel ball. The thickest part is more than 1 μm, while the tribo-film formed by ZDDP is usually about 100 nm [11]. It should be pointed out that the thickness of the tribo-film is not uniform, because the FIB system extracted the edge part of the tribo-film. In order to further analyze the microstructure of the tribo-film, the b area of Fig. 10(a) was selected for high-resolution TEM analysis. As shown in Fig. 10(b), many spherical nano-crystalline grains are embedded in the tribo-film near the steel substrate, and obvious lattice fringes can be observed. After measurement, the interplanar spacing is 0.16 nm and 0.26 nm, which correspond to the (111) and (220) faces of CeO_2 nanocrystals, respectively. Figures 10(c) and 10(d) are close-up images extracted from the c and d points in Fig. 10(a), both of which demonstrate that many nanoparticles are uniformly distributed in the tribo-film. It shows that most of the CeO_2 nanoparticles still exist in the form of CeO_2 in the tribo-film, and the CeO_2 nanoparticles are embedded in the amorphous phosphate matrix formed by ZDDP, the tribo-film of nanocomposite structure with amorphous phosphate as binder and CeO_2 nanoparticles as filling phase is formed. The nanocomposite film has higher mechanical strength and toughness [33, 34]. At the same time, $CePO_4$ makes the amorphous phase and crystalline phase combine more closely, so the tribo-film has higher load-carrying capacity.

In order to analyze the change of element content in tribo-film, EDS linear scanning was carried out in the c area of Fig. 8(a), and the scanning direction was from Pt protective layer to steel substrate. The results of linear scanning were given in Figs. 10(e) and 10(f). The content of P, Ce, and O in the tribo-film near the steel substrate and Pt protective layer is higher, which indicates that the phosphate and CeO_2 nanoparticles

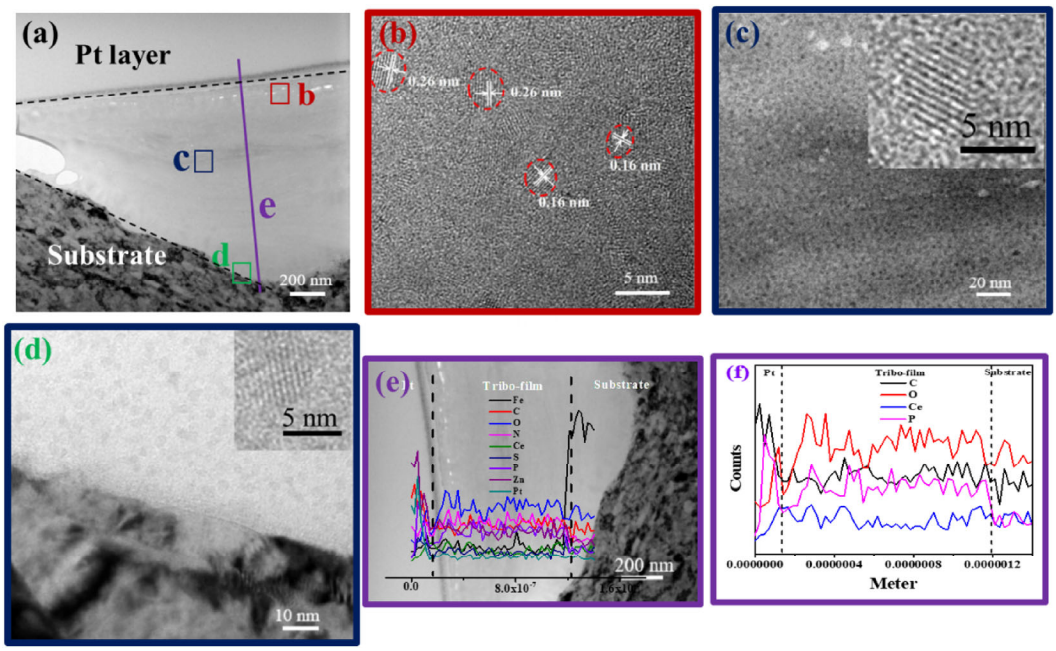

Fig. 10 TEM and EDS images of wear scar cross section of PAO6+CeO_2+ZDDP steel ball: (a) cross-section TEM image of tribo-film, (b) HRTEM image of b region tribo-film, (c) HRTEM image of c region tribo-film, (d) HRTEM image of d region tribo-film, (e) line scanning of element on worn surface, (f) line scanning of key elements inside the tribo-film (four-ball tribometer: 1,200 rpm, 392 N, 75 °C, 60 min).

have higher content in these two parts of the tribo-film. This means that ZDDP and CeO_2 nanoparticles are in a mutually beneficial coexistence state. CeO_2 nanoparticles can promote ZDDP to adsorb more on the steel surface and form a thicker phosphate tribo-film; while ZDDP can help CeO_2 nanoparticles adsorb on the steel surface faster and embed into the tribo-film earlier, so as to play a better tribological performance.

3.3.4 *Formation mechanism of tribo-film*

Figure 11 shows schematic diagrams of additives adsorbing and forming tribo-film on metal surface. As shown in Fig. 11(b), two layers of CeO_2 nanoparticles are adsorbed on the metal surface to form a loose adsorption film. The tribo-film is formed by shear induced sintering of CeO_2 nanoparticles on the metal surface, and the film forming rate is slow, which leads to low P_B value. The polar ends of ZDDP molecules are adsorbed on the metal surface, and the molecules are arranged in an orderly manner, which is a single-layer rigid adsorption, and a tribo-film composed of amorphous polyphosphate is formed by tribochemistry reaction (Fig. 11(c)). When the two additives coexist, the polar ends of some ZDDP molecules will be adsorbed on the surface of CeO_2 nanoparticles. Because the diffusion ability of small molecules is stronger than that of nanoparticles, ZDDP is preferentially adsorbed on the friction pair surface than CeO_2 nanoparticles. Subsequently, CeO_2 nanoparticles carry ZDDP molecules and continue to adsorb until the adsorption equilibrium is reached, forming a denser adsorption film of 6–8 nm,

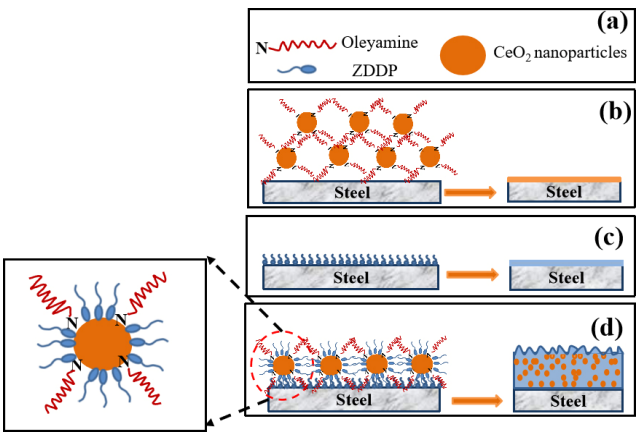

Fig. 11 Schematic diagram of the adsorption behavior of additives on the wafer: (a) additive molecules; (b) ZDDP; (c) CeO_2; (d) CeO_2+ZDDP.

so that the adsorption rate of ZDDP+CeO_2 is higher than that of any single additive. Then the P_B value of CeO_2+ZDDP is higher than that of any single additive. However, it takes nearly 2,000 s for ZDDP+CeO_2 to reach the adsorption equilibrium, which is much higher than the single shear time in the friction experiment. Therefore, the final formation of nanocomposite tribo-film of nearly 2 μm is based on the tribochemistry reaction between ZDDP and CeO_2. The tribochemistry reaction between ZDDP and CeO_2 under shear induction results in the formation of large amount of $CePO_4$, resulting in a strong adhesion between CeO_2 nanocrystals and amorphous phosphate from ZDDP induced by friction, which leads to the rapid formation of (CeO_2 nanoparticles are embedded in phosphate matrix) ultra-thick tribo-film. Due to the unique reinforcing and toughening properties of nanocomposite structure, the tribo-film with composite additives has higher load-carrying capacity.

4 Conclusions

In this paper, the composite of ZDDP and CeO_2 nano additive was used to greatly improve the adsorption rate of CeO_2 and the formation rate of tribo-film. Through the tribochemistry reaction between them, an ultra-thick tribo-film with nano-crystal CeO_2/amorphous phosphate nano-composite structure was rapidly formed on the friction surface, which not only maintains the low friction characteristics of CeO_2, but also realizes high P_B and high load-carrying capacity at the same time. The main conclusions are as follows:

(1) The thickness of the tribo-film is determined by the film forming rate and anti-wear ability of the tribo-film. Although ZDDP has high P_B value due to the high film forming rate, it has poor anti-wear ability, so it does not form a significant tribo-film. The tribo-film of CeO_2 nanoparticles has good anti-wear ability, but the film forming rate is too low, so the thickness of tribo-film is not obvious. For the compound additive of CeO_2 and ZDDP, its tribo-film has high film forming rate and anti-wear performance at the same time. In the growth stage of tribo-film, the growth rate of tribo-film is much higher than its wear rate, which leads to the rapid formation of

ultra-thick tribo-film, and finally stabilized at the thickness of 2 μm.

(2) Through the QCM adsorption experiment, it is found that the P_B value of additive has nothing to do with its equilibrium adsorption mass, but is directly proportional to its adsorption rate in 10 s. The compound additive of CeO_2 and ZDDP presents the co-deposition mode of ZDDP monolayer rigid adsorption and CeO_2 viscoelastic adsorption on the metal surface, which showed the highest adsorption rate in 10 s. Finally, it shows the maximum P_B value.

(3) The load-carrying capacity of the additive is not only related to the equilibrium adsorption mass, but also affected by the microstructure of the tribo-film. CeO_2 nanoparticles and composite additive of CeO_2 and ZDDP have the same equilibrium adsorption mass, but the latter has a higher load capacity, which is related to the formation of better nano-composite tribo-film. CeO_2 nanoparticles and ZDDP are combined to form an ultra-thick nanocomposite tribo-film with phosphate as binder and CeO_2 nanoparticles as filling phase. The tribochemistry reaction between CeO_2 nanoparticles and ZDDP results in the formation of $CePO_4$, which improves the binding force between the filler phase and the binder, and makes the structure of tribo-film more stable. This kind of nanocomposite structure tribo-film has more excellent load-carrying capacity.

Acknowledgements

We acknowledge the financial support provided by the National Natural Science Foundation of China (Nos. 51875172 and 51775168), Scientific and Technological Innovation Team of Henan Province Universities (No. 19IRTSTHN024), and Zhongyuan Science and Technology Innovation Leadership Program (No. 214200510024).

Electronic Supplementary Material: Supplementary material is available in the online version of this article at https://doi.org/10.1007/s40544-021-0571-8.

References

[1] Bhaumik S, Maggirwar R, Datta S, Pathak S D. Analyses of anti-wear and extreme pressure properties of castor oil with zinc oxide nano friction modifiers. *Appl Surf Sci* **449**: 277–286 (2018)

[2] Verma D, Kumar B, Kavita, Rastogi R B. Zinc oxide- and magnesium-doped zinc oxide-decorated nanocomposites of reduced graphene oxide as friction and wear modifiers. *ACS Appl Mater Interfaces* **11**(2): 2418–2430 (2019)

[3] Chen G Y, Zhao J, Chen K, Liu S Y, Zhang M Y, He Y Y, Luo J B. Ultrastable lubricating properties of robust self-repairing tribofilms enabled by in situ-assembled polydopamine nanoparticles. *Langmuir* **36**(4): 852–861 (2020)

[4] Liu C X, Friedman O, Meng Y G, Tian Y, Golan Y. CuS nanoparticle additives for enhanced ester lubricant performance. *ACS Appl Nano Mater* **1**(12): 7060–7065 (2018)

[5] Liu C X, Friedman O, Li Y Z, Li S W, Tian Y, Golan Y, Meng Y G. Electric response of CuS nanoparticle lubricant additives: The effect of crystalline and amorphous octadecylamine surfactant capping layers. *Langmuir* **35**(48): 15825–15833 (2019)

[6] Kumara C, Leonard D N, Meyer H M, Luo H M, Armstrong B L, Qu J. Palladium nanoparticle-enabled ultrathick tribofilm with unique composition. *ACS Appl Mater Interfaces* **10**(37): 31804–31812 (2018)

[7] Khare H, Lahouij I, Jackson A, Feng G, Chen Z Y, Cooper G D, Carpick R W. Nanoscale generation of robust solid films from liquid-dispersed nanoparticles via *in situ* atomic force microscopy: Growth kinetics and nanomechanical properties. *ACS Appl Mater Interfaces* **10**(46): 40335–40347 (2018)

[8] Zhao J, Mao J Y, Li Y R, He Y Y, Luo J B. Friction-induced nano-structural evolution of graphene as a lubrication additive. *Appl Surf Sci* **434**: 21–27 (2018)

[9] Wang B G, Tang W W, Lu H S, Huang Z Y. Ionic liquid capped carbon dots as a high-performance friction-reducing and antiwear additive for poly(ethylene glycol). *J Mater Chem A* **4**(19): 7257–7265 (2016)

[10] Shi J, Wang Y F, Gong Z B, Zhang B, Wang C B, Zhang J Y. Nanocrystalline graphite formed at fullerene-like carbon film frictional interface. *Adv Mater Interfaces* **4**(8): 1601113 (2017)

[11] Guo W, Zhou Y, Sang X H, Leonard D N, Qu J, Poplawsky J D. Atom probe tomography unveils formation mechanisms of wear-protective tribofilms by ZDDP, ionic liquid, and their combination. *ACS Appl Mater Interfaces* **9**(27): 23152–23163 (2017)

[12] Mosey N J, Müser M H, Woo T K. Molecular mechanisms for the functionality of lubricant additives. *Science* **307**(5715): 1612–1615 (2005)

[13] Gosvami N N, Bares J A, Mangolini F, Konicek A R, Yablon D G, Carpick R W. Mechanisms of antiwear tribofilm growth revealed *in situ* by single-asperity sliding contacts. *Science* **348**(6230): 102–106 (2015)

[14] Guo Z Q, Zhang Y J, Wang J C, Gao C P, Zhang S M, Zhang P Y, Zhang Z J. Interactions of Cu nanoparticles with conventional lubricant additives on tribological performance and some physicochemical properties of an ester base oil. *Tribol Int* **141**: 105941 (2020)

[15] Aldana P U, Vacher B, Mogne T, Belin M, Thiebaut B, Dassenoy F. Action mechanism of WS_2 nanoparticles with ZDDP additive in boundary lubrication regime. *Tribol Lett* **56**(2): 249–258 (2014)

[16] Wu H X, Qin L G, Zeng Q F, Dong G N. Understanding the physical adsorption action mechanism of MoS_2 nanoparticles in boundary lubrication with different polyisobutyleneamine succinimide (PIBS) concentrations. *Tribol Lett* **60**(2): 26 (2015)

[17] Wu L L, Lei X, Zhang Y J, Zhang S M, Yang G B, Zhang P Y. The tribological mechanism of cerium oxide nanoparticles as lubricant additive of poly-alpha olefin. *Tribol Lett* **68**(4): 101 (2020)

[18] Cui M, Duan Y H, Ma Y Y, Al-Shwafy K W A, Liu Y D, Zhao X D, Huang R L, Qi W, He Z M, Su R X. Real-time QCM-D monitoring of the adsorption–desorption of expansin on lignin. *Langmuir* **36**(16): 4503–4510 (2020)

[19] Meléndrez D, Jowitt T, Iliut M, Verre A F, Goodwin S, Vijayaraghavan A. Adsorption and binding dynamics of graphene-supported phospholipid membranes using the QCM-D technique. *Nanoscale* **10**(5): 2555–2567 (2018)

[20] Zhang J, Spikes H. On the mechanism of ZDDP antiwear film formation. *Tribol Lett* **63**(2): 24 (2016)

[21] Spikes H. The history and mechanisms of ZDDP. *Tribol Lett* **17**(3): 469–489 (2004)

[22] Jiang Z Q, Zhang Y J, Yang G B, Gao C P, Yu L G, Zhang S M, Zhang P Y. Synthesis of oil-soluble WS_2 nanosheets under mild condition and study of their effect on tribological properties of poly-alpha olefin under evaluated temperatures. *Tribol Int* **138**: 68–78 (2019)

[23] Kato H, Komai K. Tribofilm formation and mild wear by tribo-sintering of nanometer-sized oxide particles on rubbing steel surfaces. *Wear* **262**(1–2): 36–41 (2007)

[24] Dawczyk J, Ware E, Ardakani M, Russo J, Spikes H. Use of FIB to study ZDDP tribofilms. *Tribol Lett* **66**(4): 1–8 (2018)

[25] Nicholls M A, Do T, Norton P R, Kasrai M, Bancroft G M. Review of the lubrication of metallic surfaces by zinc dialkyl-dithiophosphates. *Tribol Int* **38**(1): 15–39 (2005)

[26] Hu Y, Jin J, Han Y Y, Yin J H, Jiang W, Liang H J. Study of fibrinogen adsorption on poly(ethylene glycol)-modified surfaces using a quartz crystal microbalance with dissipation and a dual polarization interferometry. *RSC Adv* **4**(15): 7716 (2014)

[27] Thavorn J, Hamon J J, Kitiyanan B, Striolo A, Grady B P. Competitive surfactant adsorption of AOT and TWEEN 20 on gold measured using a quartz crystal microbalance with dissipation. *Langmuir* **30**(37): 11031–11039 (2014)

[28] Zhang J, Meng Y G, Tian Y, Zhang X J. Effect of concentration and addition of ions on the adsorption of sodium dodecyl sulfate on stainless steel surface in aqueous solutions. *Colloids Surf A Physicochem Eng Aspects* **484**: 408–415 (2015)

[29] Shen T J, Wang D X, Yun J, Liu Q L, Liu X H, Peng Z X. Tribological properties and tribochemical analysis of nano-cerium oxide and sulfurized isobutene in titanium complex grease. *Tribol Int* **93**: 332–346 (2016)

[30] Topolovec-Miklozic K, Forbus T R, Spikes H A. Film thickness and roughness of ZDDP antiwear films. *Tribol Lett* **26**(2): 161–171 (2007)

[31] Hu J J, Li H, Li J L, Yan C Q, Kong J, Wu Q J, Xiong D S. Super-hard and tough $Ta_{1-x}W_xCy$ films deposited by magnetron sputtering. *Surf Coat Technol* **400**: 126207 (2020)

[32] Marchin N, Ashrafizadeh F. Effect of carbon addition on tribological performance of TiSiN coatings produced by cathodic arc physical vapour deposition. *Surf Coat Technol* **407**: 126781 (2021)

[33] Zhang R F, Veprek S. Phase stabilities of self-organized nc-TiN/a-Si_3N_4 nanocomposites and of $Ti_{1-x}Si_xN_y$ solid solutions studied by *ab initio* calculation and thermodynamic modeling. *Thin Solid Films* **516**(8): 2264–2275 (2008)

[34] Veprek S, Zhang R F, Veprek-Heijman M G J, Sheng S H, Argon A S. Superhard nanocomposites: Origin of hardness enhancement, properties and applications. *Surf Coat Technol* **204**(12–13): 1898–1906 (2010)

Xue LEI. She received her master degree in Engineering Research Center for Nanomaterials in 2021 from Henan University, Kaifeng, China. Her research interests include preparation of nano additives and the synergistic mechanism between nano additives and engine oil additives.

Yujuan ZHANG. She received her Ph.D. degree in the State key Laboratory of Solid Lubrication from Lanzhou Institute of Chemical Physics, Chinese Academy of Sciences, China, in 2005. She joined the National & Local Joint Engineering Research Center for Applied Technology of Hybrid Nanomaterials at Henan University from 2001. Her current position is a professor. Her research areas cover the tribology of solid lubricating coatings, large-scale production and industrial application of nano additives.

Shengmao ZHANG. He received his Ph.D. degree in the State key Laboratory of Solid Lubrication from Lanzhou Institute of Chemical Physics, Chinese Academy of Sciences, China, in 2005. He joined the National & Local Joint Engineering Research Center for Applied Technology of Hybrid Nanomaterials at Henan University from 2001. His current position is a professor. His research areas cover the large-scale production and industrial application of nano materials.